MIT Open Access Articles

High-resolution 17O NMR spectroscopy of structural water

The MIT Faculty has made this article openly available. ***Please share*** how this access benefits you. Your story matters.

Citation	Keeler, Eric G., et al., "High-resolution 17O NMR spectroscopy of structural water." Journal of Physical Chemistry B 123, 14 (2019): p. 3061-67 doi 10.1021/ACS.JPCB.9B02277 ©2019 Author(s)
As Published	10.1021/ACS.JPCB.9B02277
Publisher	American Chemical Society (ACS)
Version	Author's final manuscript
Citable link	https://hdl.handle.net/1721.1/125937
Terms of Use	Article is made available in accordance with the publisher's policy and may be subject to US copyright law. Please refer to the publisher's site for terms of use.

Massachusetts Institute of Technology

DSpace@MIT

Author Manuscript

Author Manuscript

Author Manuscript

Author Manuscript

HHS Public Access

Author manuscript

J Phys Chem B. Author manuscript; available in PMC 2019 August 10.

Published in final edited form as:

J Phys Chem B. 2019 April 11; 123(14): 3061–3067. doi:10.1021/acs.jpcb.9b02277.

High Resolution ^{17}O NMR Spectroscopy of Structural Water

Eric G. Keeler[1,2,§], **Vladimir K. Michaelis**[1,2,†], **Christopher B. Wilson**[2,3,‡], **Ivan Hung**[4], **Xiaoling Wang**[4,‡], **Zhehong Gan**[4], **Robert G. Griffin**[1,2,*]

[1]Department of Chemistry, Massachusetts Institute of Technology, Cambridge, Massachusetts, 02139 USA

[2]Francis Bitter Magnet Laboratory, Massachusetts Institute of Technology, Cambridge, Massachusetts, 02139 USA

[3]Department of Physics, Massachusetts Institute of Technology, Cambridge, Massachusetts, 02139 USA

[4]National High Magnetic Field Laboratory, Florida State University, Tallahassee, Florida 32310, United States

Abstract

The importance of studying site-specific interactions of structurally similar water molecules in complex systems is well known. We demonstrate the ability to resolve four distinct bound water environments within the crystal structure of lanthanum magnesium nitrate hydrate via ^{17}O solid state nuclear magnetic resonance (NMR) spectroscopy. The approach utilizes high-resolution multi-dimensional ^{17}O NMR experiments at high magnetic fields (18.8 – 35.2 T) where each individual water environment was resolved. The quadrupolar coupling constants and asymmetry parameters of the ^{17}O of each water were determined to be between 6.6 and 7.1 MHz, and 0.83 and 0.90. The resolution of the four unique, yet similar, structural waters within a hydrated crystal via ^{17}O NMR spectroscopy demonstrates the ability to decipher the unique electronic environment of structural water within a single hydrated crystal structure.

Graphical Abstract

[*]**Corresponding Author** Robert G. Griffin, rgg@mit.edu.
[§]**Present Addresses** Department of Chemistry, Columbia University, New York, New York, 10027 USA
[†]Department of Chemistry, University of Alberta, Edmonton, Alberta, T6G 2G2 Canada
[‡]Department of Physics, University of California, Santa Barbara, Santa Barbara, California, 93160 USA

No competing financial interests have been declared.

Author Manuscript Author Manuscript Author Manuscript Author Manuscript

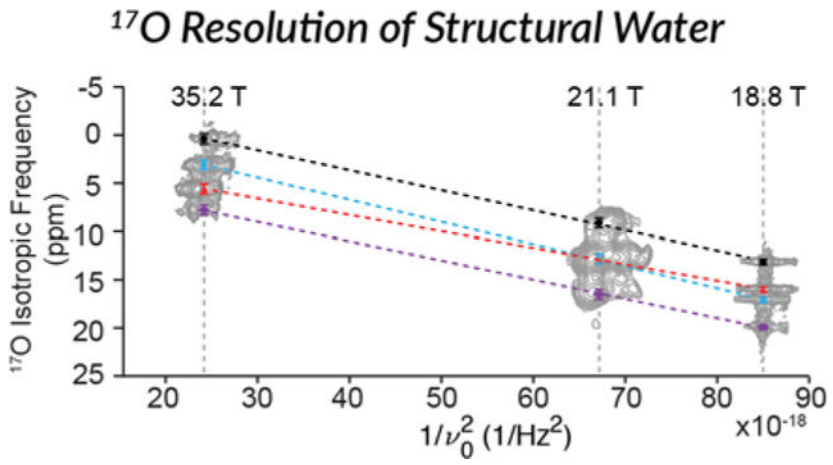

INTRODUCTION

The influence of water on the structure, stability, function, and dynamics of complex biological and inorganic systems underlines the importance of understanding the detailed structure of individual water molecules in such systems.[1] For example, it is well known that water is intimately involved in the intra- and intermolecular hydrogen bonding of proteins, membranes, and nucleic acids[2–4] and is therefore important in determining the secondary and tertiary structure of these macromolecular systems. Recently, in a combined cryo-electron microscopy and magic-angle spinning (MAS) NMR study of the structure of amyloid fibrils from our group, we observed a water bilayer that is thought to be essential to stabilizing the structure of the paired twisted β-sheets.[5–10] In addition to the impact of water on the structure of biochemical systems water is known to influence other systems,[11–19] one such system in particular is the formation of organic rosette nanotubes.[18–19] These and other results have stimulated the study of the structure of water in multiple different systems using solid-state NMR[10, 19–27] with many studies focusing on the mobile waters of hydration. However, the resolution of different water molecules, and therefore the site-specific study of these waters, has proved challenging because of the small chemical shift range present in ^{1}H NMR spectra which is the primary probe of the water molecules.[10, 20–25] In contrast, the sizeable chemical shift range (~2,000 ppm) and quadrupolar nature of ^{17}O (I = 5/2) makes it attractive for the study of intra- and intermolecular hydrogen bonding interactions involving water. However, ^{17}O NMR is inherently insensitive due to the low natural abundance (~0.037%) and small gyromagnetic ratio (~1/7th of ^{1}H). In addition, ^{17}O NMR spectra are broadened by the second-order quadrupolar interaction which is not averaged by MAS.[28] Despite these shortcomings, ^{17}O has been used extensively to study biological and inorganic systems, by utilizing isotopic enrichment,[29–33] and high magnetic field strengths (≥ 16.4 T).[34–39] Approaches improving the resolution of ^{17}O MAS NMR spectra by attenuating the second-order quadrupolar interaction, such as multiple quantum MAS (MQMAS)[40] and satellite transition MAS (STMAS),[41] have been shown to yield well-resolved isotropic quadrupolar spectra. And, despite the poor efficiency (~5%) of these techniques in the presence of large quadrupolar coupling constants (>5 MHz),[42–43] they are used to successfully study ^{17}O enriched biological samples and produced promising results.[44–47] For

Author Manuscript Author Manuscript Author Manuscript Author Manuscript

example, the increased resolution that is present in the MQMAS experiment allowed studies of inorganic glasses and minerals that could not be achieved with traditional MAS experiments.[32–33, 48–58]

In recent studies of $H_2{}^{17}O$ structurally bound to organic and inorganic crystals,[11, 59–60] we observed ^{17}O chemical shifts dispersed over ~50 ppm. This result suggests that ^{17}O NMR can be used to distinguish bound water in complex biological and inorganic systems via the dispersion of oxygen chemical shifts. Here we report ^{17}O spectra of lanthanum magnesium nitrate hydrate [$La_2Mg_3(NO_3)_{12} \cdot 24H_2{}^{17}O$] (LMN), a hydrated crystal containing four distinct water environments (each site comprised of six individual equivalent waters),[61] as a model system that demonstrates this possibility. As illustrated in Figure 1, each of the three Mg^{2+} ions is coordinated to six water molecules and the remaining waters in the crystal exist in a layer between the lanthanum nitrate and one of the magnesium hydrate subunits. The four crystallographically distinct waters are indicated on the molecular unit in Figure 1(a) with the average O-H bond distance and ∠HOH angle for each water site given in Figure 1(b).

EXPERIMENTAL

a.) Materials and Synthesis:

Lanthanum magnesium nitrate hydrate, $La_2Mg_3(NO_3)_{12} \cdot 24H_2{}^{17}O$, samples were synthesized by dissolving lanthanum nitrate hexahydrate, $La(NO_3)_3 \cdot 6H_2O$ (Sigma Aldrich (SA), St. Louis, MO), and magnesium nitrate hexahydrate, $Mg(NO_3)_2 \cdot 6H_2O$ (SA), in excess ^{17}O labeled water (90%-$H_2{}^{17}O$, Cambridge Isotopes Laboratories (CIL), Andover, MA), and recrystallizing in a sealed eppendorf tube over the course of two to 14 days. The crystals were then air-dried and ground into a fine powder using an agate mortar and pestle.

b.) Nuclear Magnetic Resonance Spectroscopy

Oxygen-17 NMR experiments were performed at 18.8 (Francis Bitter Magnet Laboratory – Massachusetts Institute of Technology, FBML-MIT), 18.8 (National High Magnetic Field Laboratory, NHMFL), and 21.1 (FBML-MIT) T using a Bruker Avance II or III spectrometer. Oxygen-17 NMR experiments were also performed at 35.2 T on the series-connected hybrid magnet at the NHFML using a Bruker Avance NEO console and a single-resonance 3.2 mm MAS probe designed and constructed at the NHMFL.[62] A recycle delay of between 0.5 and 1 second was used for all ^{17}O experiments, unless otherwise noted. Between 2,400 and 8,192 scans with $\gamma B_1/2\pi$ (^{17}O) = 27.7 to 140 kHz were utilized for MAS ^{17}O NMR experiments. A spinning frequency ($\omega_R/2\pi$) of 20 kHz or 23 kHz was used for ^{17}O MAS experiments at 18.8, and 21.1 T, respectively. One-dimensional MAS NMR experiments were acquired using a Hahn-echo ($\pi/2$–τ–acquire) pulse sequence.

Two-dimensional ^{17}O shifted-echo triple quantum magic-angle spinning (3QMAS) spectra were acquired at 18.8, 21.1, and 35.2 T with 128, 92, 44 (80) rotor-synchronized t_1 increments with an increment of 62.5, 43.48, and 100 μs with 2,016, 2,400, and 1,152 (960) scans and $\omega_R/2\pi$ = 16, 23, and 10 kHz. The 3QMAS experiments at 18.8 and 35.2 T were performed with 3Q excitation and conversion pulses of 3 and 1 μs ($\gamma B_1/2\pi$ = 100 kHz), and

Author Manuscript Author Manuscript Author Manuscript Author Manuscript

$\pi/2$ and π pulses of 2.5 and 5 μs ($\gamma B_1/2\pi$ = 33.3 kHz). The 3QMAS experiment at 21.1 T were performed with 3Q excitation and conversion pulses of 4.6 and 2.8 μs ($\gamma B_1/2\pi$ = 27.7 kHz), and $\pi/2$ and π pulses of 3 and 6 μs ($\gamma B_1/2\pi$ = 27.7 kHz). Spectra were referenced to liquid water, ^{17}O (18% $H_2{}^{17}O$, 0 ppm), via the substitution method.[63]

c.) Spectral Processing and Simulations

All spectra were processed by RNMR (Dr. D. Ruben, FBML-MIT), TOPSPIN (Bruker, Billerica, USA), or MATLAB (MathWorks, Natick, MA, USA) with between 10 and 500 Hz of exponential apodization. ^{17}O spectral simulations were performed using either the WSolids,[64] DMFit,[65] or SIMPSON[66] software packages.

RESULTS AND DISCUSSION

At high magnetic fields (18.8, 21.1, and 35.2 T[62]) multiple unique bound water environments were identified by ^{17}O NMR spectroscopy of a crystalline sample of LMN prepared from $H_2{}^{17}O$. The 3QMAS spectra illustrated in Figure 2 reveal four resolved peaks in the 2D landscape corresponding to four unique bound waters within the LMN crystals. The projection of the isotropic dimension at 18.8 T was found to have an *integrated intensity ratio* of 1:1:1:1 for the four environments (Figure 3) suggesting that they are the same bound water species that were identified by neutron diffraction.[61] The observed isotropic frequency of the MQMAS spectrum is a linear combination of the isotropic chemical shift and the 2nd order quadrupolar shift. However, while the chemical shifts increase as $\omega_0/2\pi$, the 2nd order quadrupolar shifts[28] decrease as $(1/(\omega_0/2\pi)^2)$ resulting in a change in the relative isotropic frequencies in spectra recorded at different static magnetic fields (Figure 4). There are also differences in the breadth of the peaks in the isotropic dimension that could arise from differences in structural heterogeneity or T_2 relaxation arising from the molecular motions (twofold flips) of the different environments.

The resolution of multiple water environments with such a small chemical shift difference demonstrates the ability to use ^{17}O NMR to study bound water in complex systems where the water environments are expected to be similar. The MQMAS spectrum at 21.1 T, Figure S1, shows only three resolved peaks. The field dependence of the 2nd order quadrupolar shift that causes the two center peaks that are resolved at 18.8 and 35.2 T to be nearly indistinguishable at 21.1 T (Figure 4). The determined ratio of the three peaks is 1:2:1, which is in line with the expected ratio considering that the center peak is two unresolved water environments. Using iterative spectral simulations of the 3Q-filtered MAS lineshape of each of the four peaks, the electric field gradient (EFG) and chemical shift anisotropy (CSA) tensor parameters were determined and are given in Table 1.

The breadth and asymmetry of the second-order quadrupolar lineshape of the central transition of half-integer quadrupolar nuclei, as measured by the quadrupole coupling constant, C_Q, and the asymmetry parameter, η_Q, depend on the local structure of the oxygen nucleus. Therefore, the differences in the EFG and CSA tensor parameters could yield a better understanding of the structure of each of the water environments.

Author Manuscript Author Manuscript Author Manuscript Author Manuscript

The quadrupole coupling constants were found to be between 6.6 and 7.1 MHz. Although previous work has shown that the asymmetry parameter is a sensitive indicator of the ∠HOH bond angle,[67] the fast limit twofold flipping of the bound water in the fast limit at room temperature averages the EFG tensor,[11, 59–60] rendering the ability to use the asymmetry parameter as a target for assignment of the water environments is ill-advised. The experimentally determined asymmetry parameters for the four water environments in LMN were found to be between 0.83 and 0.9. The differences found in the EFG tensors likely reflect both differences in the local structure and the room temperature dynamics of the bound waters. Both the EFG and CSA tensor values were found to be in good agreement with previous results for bound water within hydrated crystals.[11, 59–60] While the one-dimensional MAS NMR spectra at 18.8 and 21.1 T (Figure 5) indicated the presence of multiple unique oxygen environments, the 2D MQMAS experiments were necessary to identify and characterize the four oxygen environments (Figures 2 and 5). Although inclusion of the ^{17}O chemical shift parameters did not affect the 1D MAS NMR lineshape, it was necessary to include the CSA tensor parameters (Table 1) for the simulations of the 3QMAS lineshapes at 35.2 T (Figure 6). The 3QMAS dimension was analyzed from the projection of the direct dimension of the 2D MQMAS experiment.

Unique assignments of the NMR resolved peaks to the crystal structure water environments were not performed in this study due to the complex dynamics of such environments.[11, 59–60, 68–70] The librational modes of the bound water sites have been shown to average the EFG tensors and therefore complicate the relationship between local and hydrogen bonding structure and the experimentally determined EFG tensors at room temperature. While a dependence of the isotropic chemical shift and the OH bond distance and ∠HOH bond angle was reported in crystalline amino acid and dipeptide hydrates,[60] a study of crystalline inorganic hydrates did not demonstrate the same dependence.[11] Either correlation spectroscopy between the ^{17}O and nearby nuclei or low temperature NMR could be utilized to assist in determining which NMR environments correspond to their neutron diffraction counterparts.

CONCLUSION

Notwithstanding a unique assignment of the $H_2{}^{17}O$ lines, the resolution of multiple structurally similar environments indicates the benefit of high magnetic fields for the study of structurally important bound water. Due to the nature of the crystal structure studied here, correlation spectroscopy (e.g., ^{13}C-^{17}O, ^{15}N-^{17}O)[47, 71–74] was not performed to better identify the oxygen environments that were resolved. However for complex biological systems, such as GNNQQNY or $TTR_{105–115}$,[6–9] where more accessible correlation spectroscopy is available an identification of resolved structural water molecules may be possible. The ability to use high resolution ^{17}O MAS NMR to study unique, yet similar, structural waters in a single inorganic crystal structure indicates the possibility of analyzing structural waters in complex inorganic and biological systems. The addition of dynamic nuclear polarization to the high resolution ^{17}O MAS NMR[75–76] will enhance the ability to study the small number of structural water molecules in these complex systems in comparison to the inorganic crystal in this study.

Author Manuscript Author Manuscript Author Manuscript Author Manuscript

Supplementary Material

Refer to Web version on PubMed Central for supplementary material.

ACKNOWLEDGMENT

This work was supported by the National Institutes of Health (NIH) through grant numbers: AG058504 and EB002026. VKM is grateful to the Natural Sciences and Engineering Research Council of Canada and the Government of Canada for a Banting Postdoctoral Fellowship. Part of the work was performed at the National High Magnetic Field Laboratory supported through National Science Foundation Cooperative Agreement (DMR-1644779) and by the State of Florida. Development of the 35.2 T magnet and NMR instrumentation was supported by National Science Foundation DMR-1039938 and DMR-0603042.

Funding Sources

REFERENCES

1. Levy Y; Onuchic JN, Water and proteins: A love-hate relationship. Proceedings of the National Academy of Sciences 2004, 101, 3325–3326.
2. Glowacki ED; Irimia-Vladu M; Bauer S; Sariciftci NS, Hydrogen-bonds in molecular solids - from biological systems to organic electronics. Journal of Materials Chemistry B 2013, 1, 3742–3753.
3. Horowitz S; Trievel RC, Carbon-Oxygen Hydrogen Bonding in Biological Structure and Function. Journal of Biological Chemistry 2012, 287, 41576–41582. [PubMed: 23048026]
4. Griffin RG, Observation of the effect of water on the phosphorus-31 nuclear magnetic resonance spectra of dipalmitoyllecithin. Journal of the American Chemical Society 1976, 98, 851–853. [PubMed: 1267937]
5. Caporini MA; Bajaj VS; Veshtort M; Fitzpatrick A; MacPhee CE; Vendruscolo M; Dobson CM; Griffin RG, Accurate Determination of Interstrand Distances and Alignment in Amyloid Fibrils by Magic Angle Spinning NMR. Journal of Physical Chemistry B 2010, 114, 13555–13561.
6. Debelouchina GT; Bayro MJ; Fitzpatrick AW; Ladizhansky V; Colvin MT; Caporini MA; Jaroniec CP; Bajaj VS; Rosay M; MacPhee CE, et al., Higher Order Amyloid Fibril Structure by MAS NMR and DNP Spectroscopy. Journal of the American Chemical Society 2013, 135, 19237–19247. [PubMed: 24304221]
7. Debelouchina GT; Bayro MJ; van der Wel PCA; Caporini MA; Barnes AB; Rosay M; Maas WE; Griffin RG, Dynamic nuclear polarization-enhanced solid-state NMR spectroscopy of GNNQQNY nanocrystals and amyloid fibrils. Physical Chemistry Chemical Physics 2010, 12, 5911–5919. [PubMed: 20454733]
8. Fitzpatrick AWP; Debelouchina GT; Bayro MJ; Clare DK; Caporini MA; Bajaj VS; Jaroniec CP; Wang L; Ladizhansky V; Müller SA, et al., Atomic structure and hierarchical assembly of a cross-β amyloid fibril. Proceedings of the National Academy of Sciences 2013, 110, 5468–5473.
9. van der Wel PCA; Hu KN; Lewandowski J; Griffin RG, Dynamic nuclear polarization of amyloidogenic peptide nanocrystals: GNNQQNY, a core segment of the yeast prion protein Sup35p. Journal of the American Chemical Society 2006, 128, 10840–10846. [PubMed: 16910679]
10. Wang T; Jo H; DeGrado WF; Hong M, Water Distribution, Dynamics, and Interactions with Alzheimer's beta-Amyloid Fibrils Investigated by Solid-State NMR. Journal of the American Chemical Society 2017, 139, 6242–6252. [PubMed: 28406028]
11. Nour S; Widdifield CM; Kobera L; Burgess KMN; Errulat D; Terskikh VV; Bryce DL, Oxygen-17 NMR spectroscopy of water molecules in solid hydrates. Canadian Journal of Chemistry 2016, 94, 189–197.
12. Bell DR; Rossman GR, Water in Earths Mantle - the Role of Nominally Anhydrous Minerals. Science 1992, 255, 1391–1397. [PubMed: 17801227]
13. Benziger J; Bocarsly A; Cheah MJ; Majsztrik P; Satterfield B; Zhao Q, Mechanical and Transport Properties of Nafion: Effects of Temperature and Water Activity. Fuel Cells and Hydrogen Storage 2011, 141, 85–113.

Author Manuscript Author Manuscript Author Manuscript Author Manuscript

14. Bobylev IB; Gerasimov EG; Zyuzeva NA, Effect of structural water on the critical characteristics of highly textured $YBa_2Cu_3O_{6.9}$. Physics of the Solid State 2014, 56, 1742–1747.
15. Lebofsky LA; Feierberg MA; Tokunaga AT; Larson HP; Johnson JR, The 1.7- to 4.2-μm Spectrum of Asteroid 1 Ceres - Evidence for Structural Water in Clay-Minerals. Icarus 1981, 48, 453–459.
16. Xu WQ; Hausner DB; Harrington R; Lee PL; Strongin DR; Parise JB, Structural water in ferrihydrite and constraints this provides on possible structure models. American Mineralogist 2011, 96, 513–520.
17. Zhao QA; Majsztrik P; Benziger J, Diffusion and Interfacial Transport of Water in Nafion. Journal of Physical Chemistry B 2011, 115, 2717–2727.
18. Yamazaki T; Fenniri H; Kovalenko A, Structural Water Drives Self-assembly of Organic Rosette Nanotubes and Holds Host Atoms in the Channel. Chemphyschem 2010, 11, 361–367. [PubMed: 20017180]
19. Fenniri H; Tikhomirov GA; Brouwer DH; Bouatra S; El Bakkari M; Yan ZM; Cho JY; Yamazaki T, High Field Solid-State NMR Spectroscopy Investigation of ^{15}N-Labeled Rosette Nanotubes: Hydrogen Bond Network and Channel-Bound Water. Journal of the American Chemical Society 2016, 138, 6115–6118. [PubMed: 27141817]
20. Lesage A; Böckmann A, Water-protein interactions in microcrystalline Crh measured by ^{1}H-^{13}C solid-state NMR spectroscopy. Journal of the American Chemical Society 2003, 125, 13336–13337. [PubMed: 14583011]
21. Lesage A; Emsley L; Penin F; Böckmann A, Investigation of dipolar-mediated water-protein interactions in microcrystalline Crh by solid-state NMR spectroscopy. Journal of the American Chemical Society 2006, 128, 8246–8255. [PubMed: 16787089]
22. Luo WB; Hong M, Conformational Changes of an Ion Channel Detected Through Water-Protein Interactions Using Solid-State NMR Spectroscopy. Journal of the American Chemical Society 2010, 132, 2378–2384. [PubMed: 20112896]
23. Sergeyev IV; Bahri S; Day LA; McDermott AE, Pf1 bacteriophage hydration by magic angle spinning solid-state NMR. Journal of Chemical Physics 2014, 141.
24. White PB; Wang T; Park YB; Cosgrove DJ; Hong M, Water-Polysaccharide Interactions in the Primary Cell Wall of Arabidopsis thaliana from Polarization Transfer Solid-State NMR. Journal of the American Chemical Society 2014, 136, 10399–10409. [PubMed: 24984197]
25. Mandala VS; Gelenter MD; Hong M, Transport-Relevant Protein Conformational Dynamics and Water Dynamics on Multiple Time Scales in an Archetypal Proton Channel: Insights from Solid-State NMR. Journal of the American Chemical Society 2018, 140, 1514–1524. [PubMed: 29303574]
26. Shi LC; Kawamura I; Jung KH; Brown LS; Ladizhansky V, Conformation of a Seven-Helical Transmembrane Photosensor in the Lipid Environment. Angewandte Chemie International Edition 2011, 50, 1302–1305. [PubMed: 21290498]
27. Wilson EE; Awonusi A; Morris MD; Kohn DH; Tecklenburg MMJ; Beck LW, Three structural roles for water in bone observed by solid-state NMR. Biophysical Journal 2006, 90, 3722–3731. [PubMed: 16500963]
28. Grandinetti PJ; Trease NM; Ash JT, Symmetry Pathways in Solid State NMR. Progress in Nuclear Magnetic Resonance Spectroscopy 2011, 59, 121–196. [PubMed: 21742158]
29. Wong A; Poli F, Solid-State 17O NMR Studies of Biomolecules. Annual Reports on NMR Spectroscopy 2014, 83, 145–220.
30. Wu G, Solid-State ^{17}O NMR Studies of Organic and Biological Molecules. Progress in Nuclear Magnetic Resonance Spectroscopy 2008, 52, 118–169.
31. Wu G, Oxygen 17 NMR Studies of Organic and Biological Molecules In eMagRes, John Wiley & Sons, Ltd: Chichester, UK, 2011 10.1002/9780470034590.emrstm1212.
32. Ashbrook SE; Smith ME, Solid state ^{17}O NMR - An introduction to the background principles and applications to inorganic materials. Chemical Society Reviews 2006, 35, 718–735. [PubMed: 16862272]
33. Ashbrook SE; Smith ME, Oxygen-17 NMR of Inorganic Materials In eMagRes, John Wiley & Sons, Ltd: Chichester, UK, 2007 10.1002/9780470034590.emrstm1213.

Author Manuscript Author Manuscript Author Manuscript Author Manuscript

34. Aguiar PM; Michaelis VK; McKinley CM; Kroeker S, Network connectivity in cesium borosilicate glasses: ^{17}O multiple-quantum MAS and double-resonance NMR. Journal of Non-Crystalline Solids 2013, 363, 50–56.
35. Kong X; Shan M; Terskikh V; Hung I; Gan Z; Wu G, Solid-State ^{17}O NMR of Pharmaceutical Compounds: Salicyclic Acid and Aspirin. Journal of Physical Chemistry B 2013, 117, 9643–9654.
36. Kwan I; Mo X; Wu G, Probing hydrogen bonding and ion-carbonyl interactions by solid-state ^{17}O NMR Spectroscopy: G-Ribbon and G-Quartet. Journal of the American Chemical Society 2007, 129, 2398–2407. [PubMed: 17269776]
37. Wu G, Solid-State ^{17}O NMR studies of organic and biological molecules: Recent advances and future directions. Solid State Nuclear Magnetic Resonance 2016, 73, 1–14. [PubMed: 26651417]
38. Zhu JF; Ye E; Terskikh V; Wu G, Solid-State ^{17}O NMR Spectroscopy of Large Protein-Ligand Complexes. Angewandte Chemie International Edition 2010, 49, 8399–8402. [PubMed: 20672261]
39. Antzutkin ON; Iuga D; Filippov AV; Kelly RT; Becker-Baldus J; Brown SP; Dupree R, Hydrogen Bonding in Alzheimer's Amyloid-β Fibrils Probed by ^{15}N{^{17}O} REAPDOR Solid-State NMR Spectroscopy. Angewandte Chemie International Edition 2012, 51, 10289–10292. [PubMed: 22976560]
40. Frydman L; Hardwood JS, Isotropic Spectra of Half-Integer Quadrupolar Spins from Bidimenstional Magic-Angle Spinning NMR. Journal of the American Chemical Society 1995, 117, 5367–5368.
41. Gan Z, Isotropic NMR Spectra of Half-Integer Quadrupolar Nuclei Using Satellite Transitions and Magic-Angle Spinning. Journal of the American Chemical Society 2000, 122, 3242–3243.
42. Wu G; Rovnyak D; Huang PC; Griffin RG, High-resolution oxygen-17 NMR spectroscopy of solids by multiple-quantum magic-angle-spinning. Chemical Physics Letters 1997, 277, 79–83.
43. Wu G; Rovnyak D; Griffin RG, Quantitative multiple-quantum magic-angle-spinning NMR spectroscopy of quadrupolar nuclei in solids. Journal of the American Chemical Society 1996, 118, 9326–9332.
44. Wong A; Howes AP; Yates JR; Watts A; Anupold T; Past J; Samoson A; Dupree R; Smith ME, Ultra-High Resolution ^{17}O Solid-State NMR Spectroscopy of Biomolecules: A Comprehensive Spectral Analysis of Monosodium L-Glutamate Monohydrate. Physical Chemistry Chemical Physics 2011, 13, 12213–12224. [PubMed: 21603686]
45. O'Dell LA; Ratcliffe CI; Kong X; Wu G, Multinuclear Solid-State Nuclear Magnetic Resonance and Density Functional Theory Characterization of Interaction Tensors in Taurine. The Journal of Physical Chemistry A 2012, 116, 1008–1014. [PubMed: 22225526]
46. Prasad S; Clark TM; Sharma R; H.T K; Grandinetti PJ; Zimmermann H, A Combined ^{17}O RAPT and MQ-MAS NMR Study of L-Leucine. Solid State Nuclear Magnetic Resonance 2006, 29, 119–124. [PubMed: 16293400]
47. Keeler EG; Michaelis VK; Colvin MT; Hung I; Gor'kov PL; Cross TA; Gan Z; Griffin RG, ^{17}O MAS NMR Correlation Spectroscopy at High Magnetic Fields. Journal of the American Chemical Society 2017, 139, 17953–17963. [PubMed: 29111706]
48. Ashbrook SE, Recent advances in solid-state NMR spectroscopy of quadrupolar nuclei. Physical Chemistry Chemical Physics 2009, 11, 6892–6905. [PubMed: 19652823]
49. Ashbrook SE; Antonijevic S; Berry AJ; Wimperis S, Motional broadening: an important distinction between multiple-quantum and satellite-transition MAS NMR of quadrupolar nuclei. Chemical Physics Letters 2002, 364, 634–642.
50. Ashbrook SE; Berry AJ; Frost DJ; Gregorovic A; Pickard CJ; Readman JE; Wimperis S, ^{17}O and ^{29}Si NMR parameters of $MgSiO_3$ phases from high-resolution solid-state NMR spectroscopy and first-principles calculations. Journal of the American Chemical Society 2007, 129, 13213–13224. [PubMed: 17924628]
51. Ashbrook SE; Berry AJ; Wimperis S, Three- and five-quantum O-17 MAS NMR of forsterite Mg_2SiO_4. American Mineralogist 1999, 84, 1191–1194.
52. Ashbrook SE; Berry AJ; Wimperis S, ^{17}O multiple-quantum MAS NMR study of high-pressure hydrous magnesium silicates. Journal of the American Chemical Society 2001, 123, 6360–6366. [PubMed: 11427061]

Author Manuscript Author Manuscript Author Manuscript Author Manuscript

53. Ashbrook SE; Berry AJ; Wimperis S, ^{17}O multiple-quantum MAS NMR study of pyroxenes. Journal of Physical Chemistry B 2002, 106, 773–778.
54. Dirken PJ; Kohn SC; Smith ME; van Eck ERH, Complete resolution of Si-O-Si and Si-O-Al fragments in an aluminosilicate glass by ^{17}O multiple quantum magic angle spinning NMR spectroscopy. Chemical Physics Letters 1997, 266, 568–574.
55. Stebbins JF; Oglesby JV; Lee SK, Oxygen sites in silicate glasses: a new view from oxygen-17 NMR. Chemical Geology 2001, 174, 63–75.
56. van Eck ERH; Smith ME; Kohn SC, Observation of hydroxyl groups by ^{17}O solid-state multiple quantum MAS NMR in sol-gel-produced silica. Solid State Nuclear Magnetic Resonance 1999, 15, 181–188. [PubMed: 10672942]
57. Lee SK; Stebbins JF; Weiss CA; Kirkpatrick RJ, ^{17}O and ^{27}Al MAS and 3QMAS NMR study of synthetic and natural layer silicates. Chemistry of Materials 2003, 15, 2605–2613.
58. Lee SK; Weiss CA, Multiple oxygen sites in synthetic phyllosilicates with expandable layers: ^{17}O solid-state NMR study. American Mineralogist 2008, 93, 1066–1071.
59. Keeler EG; Michaelis VK; Griffin RG, ^{17}O NMR Investigation of Water Structure and Dynamics. Journal of Physical Chemistry B 2016, 120, 7851–7858.
60. Michaelis VK; Keeler EG; Ong T-C; Craigen KN; Penzel SA; Wren JEC; Kroeker S; Griffin RG, Structural Insights into Bound Water in Crystalline Amino Acids: Experimental and Theoretical ^{17}O NMR. The Journal of Physical Chemistry B 2015, 119, 8024–8036. [PubMed: 25996165]
61. Anderson MR; Jenkin GT; White JW, Neutron-Diffraction Study of Lanthanum Magnesium-Nitrate La2Mg3(NO3)12•24H2O. Acta Crystallographica Section B-Structural Science 1977, 33, 3933–3936.
62. Gan Z; Hung I; Wang X; Paulino J; Wu G; Litvak IM; Gor'kov PL; Brey WW; Lendi P; Schiano JL, et al., NMR spectroscopy up to 35.2T using a series-connected hybrid magnet. Journal of Magnetic Resonance 2017, 284, 125–136. [PubMed: 28890288]
63. Harris RK; Becker ED; De Menezes SMC; Granger P; Hoffman RE; Zilm KW, Further conventions for NMR shielding and chemical shifts (IUPAC recommendations 2008). Pure and Applied Chemistry 2008, 80, 59–84.
64. Eichele K WSolids1 NMR Simulation Package, 1.20.21; 2013.
65. Massiot D; Fayon F; Capron M; King I; Le Calve S; Alonso B; Durand JO; Bujoli B; Gan ZH; Hoatson G, Modelling one- and two-dimensional solid-state NMR spectra. Magnetic Resonance in Chemistry 2002, 40, 70–76.
66. Bak M; Rasmussen JT; Nielsen NC, SIMPSON: A general simulation program for solid-state NMR spectroscopy. Journal of Magnetic Resonance 2000, 147, 296–330. [PubMed: 11097821]
67. Sternberg U, The bond angle dependence of the asymmetry parameter of the oxygen-17 electric field gradient tensor. Solid State Nuclear Magnetic Resonance 1993, 2, 181–190. [PubMed: 7827969]
68. Chiba T, Deuteron Magnetic Resonance Study of Barium Chlorate Monohydrate. Journal of Chemical Physics 1963, 39, 947–953.
69. Thaper CL; Dasannacharya BA; Sequeira A; Iyengar PK, Observation of Librational Modes of Water Molecules in Single Crystal Hydrates by Neutron Scattering. Solid State Communications 1970, 8, 497–499.
70. Long JR; Ebelhauser R; Griffin RG, ^{2}H NMR line shapes and spin-lattice relaxation in Ba(ClO3)2•2H2O. Journal of Physical Chemistry A 1997, 101, 988–994.
71. Perras FA; Chaudhary U; Slowing II; Pruski M, Probing Surface Hydrogen Bonding and Dynamics by Natural Abundance, Multidimensional, ^{17}O DNP-NMR Spectroscopy. Journal of Physical Chemistry C 2016, 120, 11535–11544.
72. Perras FA; Kobayashi T; Pruski M, Natural Abundance ^{17}O DNP Two-Dimensional and Surface-Enhanced NMR Spectroscopy. Journal of the American Chemical Society 2015, 137, 8336–8339. [PubMed: 26098846]
73. Hung I; Uldry AC; Becker-Baldus J; Webber AL; Wong A; Smith ME; Joyce SA; Yates JR; Pickard CJ; Dupree R, et al., Probing Heteronuclear ^{15}N-^{17}O and ^{13}C-^{17}O Connectivities and Proximities by Solid-State NMR Spectroscopy. Journal of the American Chemical Society 2009, 131, 1820–1834. [PubMed: 19138069]

Author Manuscript Author Manuscript Author Manuscript Author Manuscript

74. Carnahan SL; Lampkin BJ; Naik P; Hanrahan MP; Slowing II; VanVeller B; Wu G; Rossini AJ, Probing O-H Bonding Through Proton Detected ^{1}H-^{17}O Double Resonance Solid-State NMR Spectroscopy. Journal of the American Chemical Society 2018.

75. Michaelis VK; Corzilius B; Smith AA; Griffin RG, Dynamic Nuclear Polarization of ^{17}O: Direct Polarization. The Journal of Physical Chemistry B 2013, 117, 14894–14906. [PubMed: 24195759]

76. Michaelis VK; Markhasin E; Daviso E; Herzfeld J; Griffin RG, Dynamic Nuclear Polarization of Oxygen-17. The Journal of Physical Chemistry Letters 2012, 3, 2030–2034. [PubMed: 23024834]

Author Manuscript Author Manuscript Author Manuscript Author Manuscript

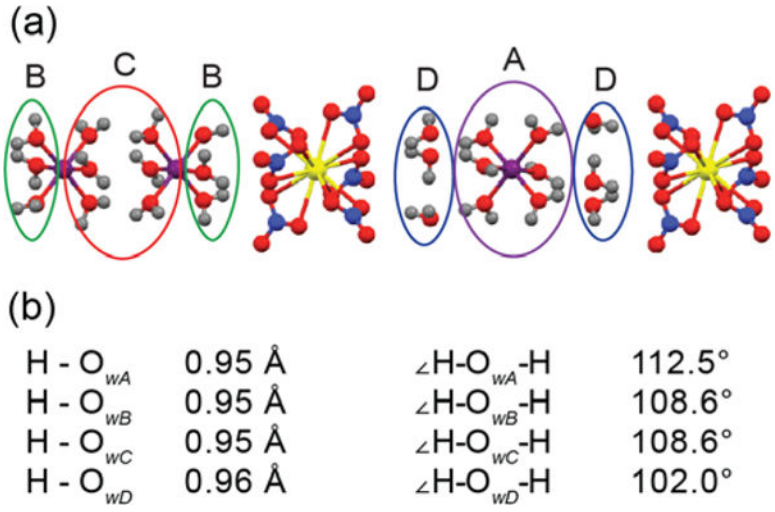

Figure 1:

LMN crystal structure (a) showing the four crystallographically distinct water environments labeled as A-D, and corresponding (b) interatomic distances and angles determined by neutron diffraction.[61]

Author Manuscript Author Manuscript Author Manuscript Author Manuscript

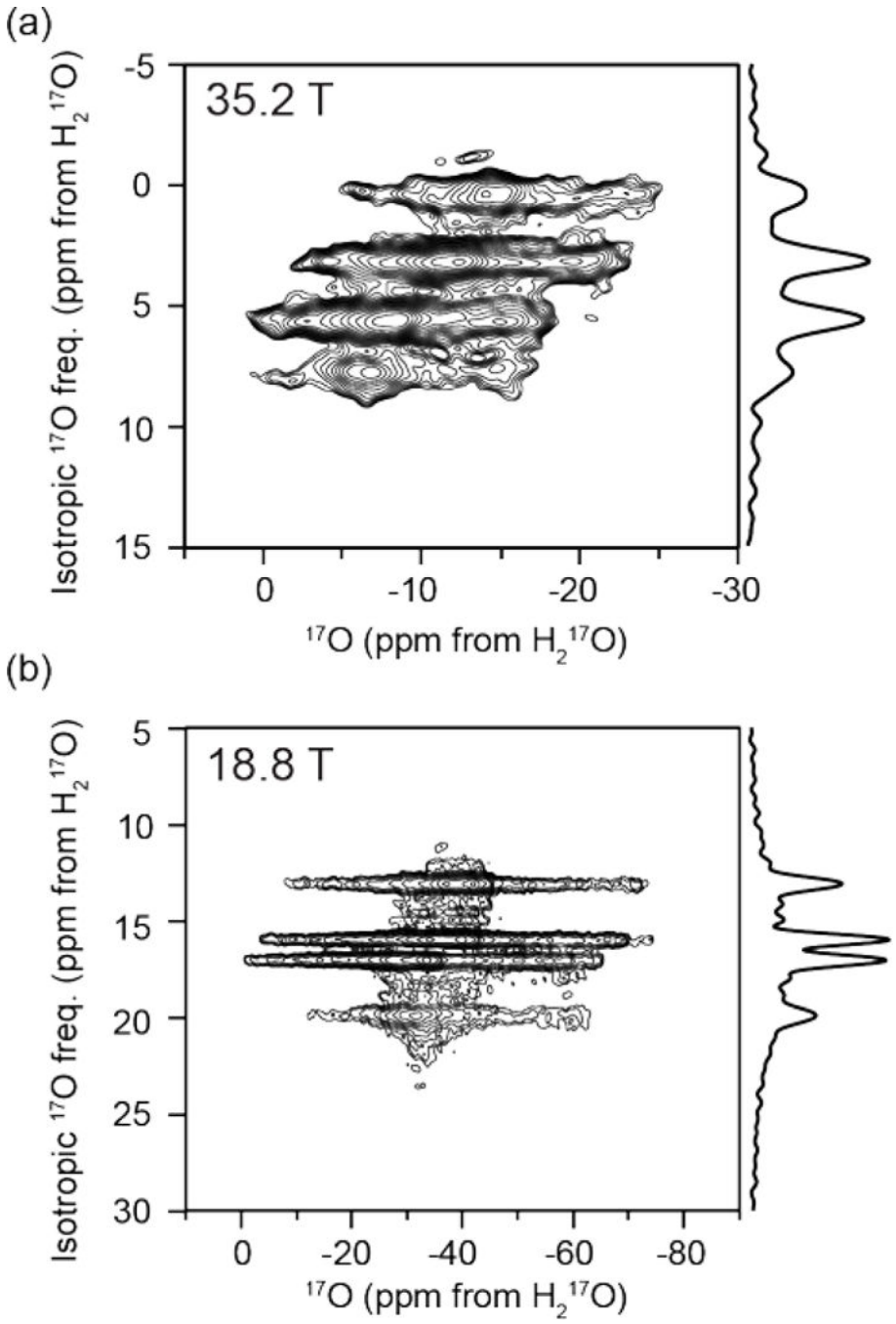

Figure 2:

Oxygen-17 2D MQMAS NMR spectra at (a) 35.2 T ($\omega_{0H}/2\pi$ = 1500 MHz) and (b) 18.8 T ($\omega_{0H}/2\pi$ = 800 MHz). Four distinct water sites are resolved in each spectrum. The projection of the isotropic dimension is shown to the right of each spectrum.

Author Manuscript Author Manuscript Author Manuscript Author Manuscript

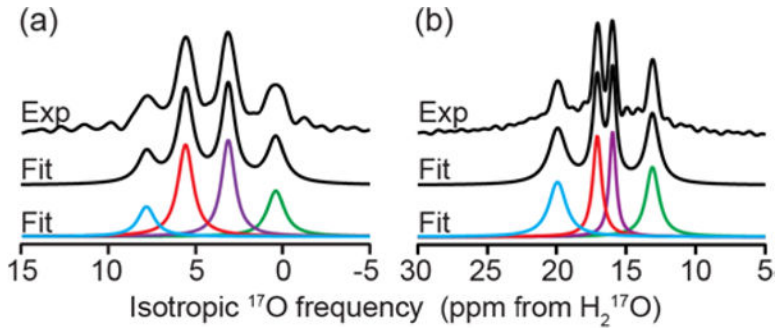

Figure 3:

Experimental and fit Isotropic projections of ^{17}O 2D MQMAS spectra at (a) 35.2 T ($\omega_{0H}/2\pi$ = 1500 MHz) and (b) 18.8 T ($\omega_{0H}/2\pi$ = 800 MHz). Four distinct water environments are resolved with isotropic frequencies of (a) 0.4 ± 1, 3.1 ± 1, 5.6 ± 1, and 7.8 ± 1 ppm and (b) 13.1 ± 1, 16.0 ± 1, 17.1 ± 1, and 19.9 ± 1 ppm. The Lorenztian fits of each environment indicate a ratio of populations of 1:1:1:1.

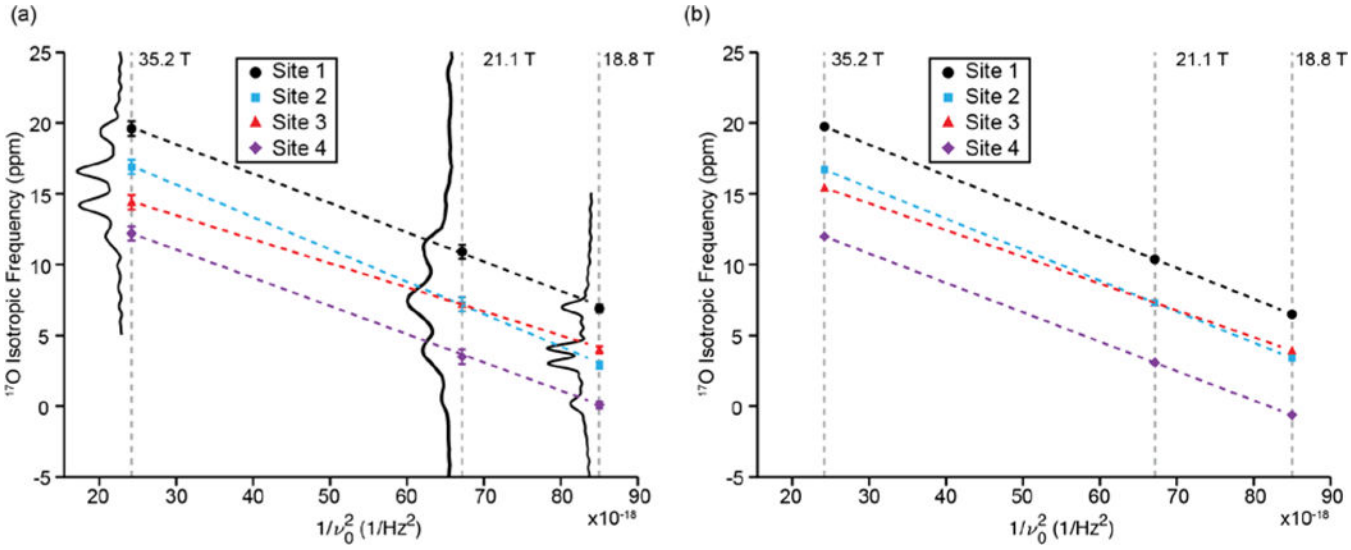

Figure 4:

Magnetic field dependence (B_o = 18.1 to 35.2 T) of the observed ^{17}O isotropic frequency shown using the (a) observed isotropic frequency from the 2D MQMAS spectra, and (b) using the equation $\delta_{iso} = \delta_{3Q} + \frac{3}{850}\frac{P_Q^2}{\nu_0^2} x10^{-6}$, where $P_Q = C_Q\sqrt{1+\frac{\eta^2}{3}}$ and ν_0 is the Larmor frequency of ^{17}O and is calculated from the values in Table 1. A projection of the isotropic dimension at each field is shown to the left of the isotropic frequencies for each field in (a). The dashed lines (Black, Red, Blue and Purple) are linear fitted lines to the isotropic frequencies of each site.

Author Manuscript Author Manuscript Author Manuscript Author Manuscript

Author Manuscript Author Manuscript Author Manuscript Author Manuscript

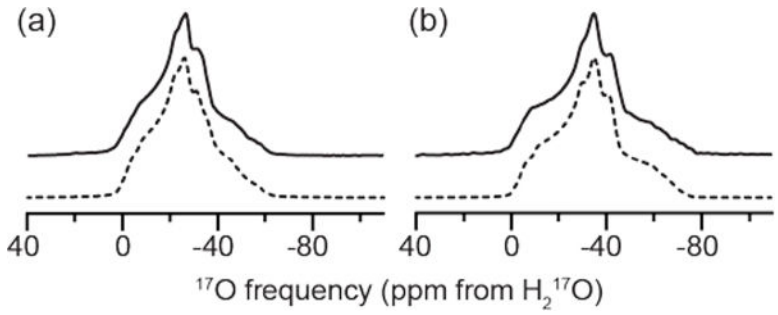

Figure 5:

Experimental (solid) and simulated (dashed) ^{17}O MAS NMR spectra at (a) 21.1 T ($\omega_{0H}/2\pi$ = 900 MHz), and (b) 18.8 T ($\omega_{0H}/2\pi$ = 800 MHz) with $\omega_R/2\pi$ = 23, and 20 kHz, respectively. EFG tensor parameters for the spectral simulations are given in Table 1.

Author Manuscript Author Manuscript Author Manuscript Author Manuscript

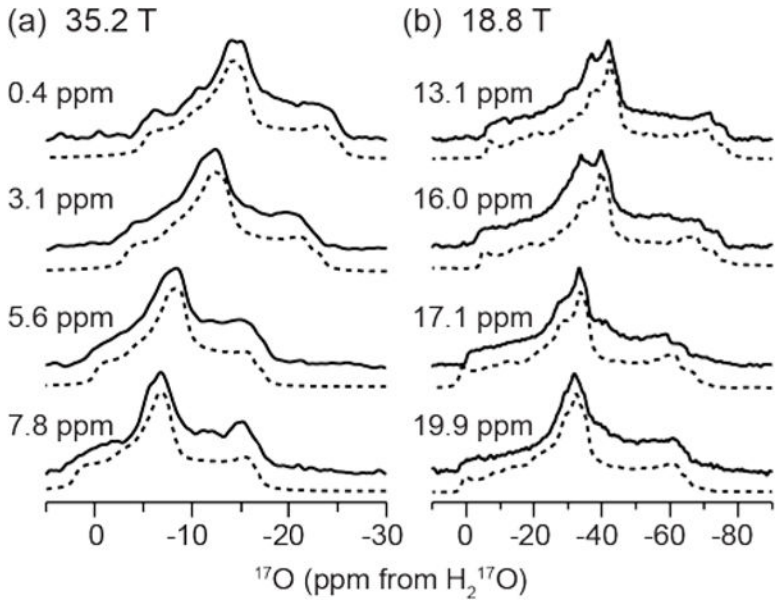

Figure 6:

Projections of the 3Q-filtered lineshape of each ^{17}O resonance from Figure 2 at (a) 35.2 T ($\omega_{0H}/2\pi$ = 1500 MHz) and (b) 18.8 T ($\omega_{0H}/2\pi$ = 800 MHz) with spectral simulations displayed as dashed lines. The EFG and CSA tensor parameters of the simulations are given in Table 1.

Author Manuscript

Author Manuscript

Author Manuscript

Author Manuscript

Table 1:

^{17}O EFG and CSA tensor parameters determined from MAS and MQMAS NMR

^{17}O site	**C_Q (± 0.3) / MHz**	**η_Q (± 0.15)**	**δ_{iso} / ppm**	**Ω (± 30) / ppm**	**κ (± 0.5)**	**δ_{3Q} (±1) / ppm at 18.8 T**	**δ_{3Q} (±1) / ppm at 21.1 T**	**δ_{3Q} (±1) / ppm at 35.2 T**
1	7.1	0.8_5	−5 ± 2	50	−1	13.1	9.1	0.4
2	7.1	0.8_3	−2 ± 2	70	−1	17.1	*n.r.*	3.1
3	6.6	0.8_3	0 ± 2	70	−1	16.0	*n.r.*	5.6
4	6.8	0.9	3 ± 2	80	−1	19.9	16.5	7.8

n.r. – not resolved, one peak at 12.8 ±1 ppm.